The favorable routes for the hydrolysis of CH_2OO with $(H_2O)_n$ (n = 1-4) investigated by global minimum searching combined with quantum chemical methods

Rui Wang[a,e], Mingjie Wen[a,e,#], Shuai Liu[a,#], Yousong Lu[b,#], Makroni Lily[b,#], Balaganesh Muthiah[d], Tianlei Zhang[a,e,*], Zhiyin Wang[a], Zhuqing Wang[c,*]

[a] *School of Chemical & Environment Science, Shaanxi University of Technology, Hanzhong, Shaanxi 723001, P. R. China*

[b] *Key Laboratory for Macromolecular Science of Shaanxi Province, School of Chemistry & Chemical Engineering, Shaanxi Normal University, Xi'an, Shaanxi 710062, P. R. China*

[c] *School of Chemical Engineering, Sichuan University of Science & Engineering, Zigong, 643000, P. R. China*

[d] *Department of Chemistry, National Taiwan University, Taipei 106, Taiwan*

[e] *Shanghai Key Laboratory of Molecular Catalysis and Innovative Materials, Fudan University, Shanghai 200433, P. R. China*

S. NO	Caption
3	**Fig. S1** Optimized geometries and the binding energy for the complexes of $(H_2O)_n$ (n = 1-4) at the CCSD(T)-F12a/cc-pVDZ-F12//B3LYP/6-311+G(2*d*,2*p*) level of theory (in kcal·mol^{-1}) (Bond distances in Angstroms and angles in degrees)
4	**Table S1** Zero point energies (ZPE/(kcal·mol^{-1})), relative energies (ΔE and $\Delta(E$+ZPE)/(kcal·mol^{-1})), enthalpies (ΔH(298K)/(kcal·mol^{-1})), entropy (S(298)/(cal·mol^{-1}·K^{-1})) and free energies (ΔG(298K)/(kcal·mol^{-1})) for the $(H_2O)_n$ (n = 2-4)[a]
5	**Fig. S2** The most stable geometry and the binding energy of $CH_2OO\cdots(H_2O)_2$ complexes searched by ABCluster program (in kcal·mol^{-1}) (Bond distances in Angstroms and angles in degrees)
6	**Fig. S3** The geometrical possible structures and the binding energy for the $CH_2OO\cdots(H_2O)_n$ (n = 1-4) complexes at the CCSD(T)-F12a/cc-pVDZ-F12//B3LYP/6-311+G(2*d*,2*p*) level of theory (in kcal·mol^{-1}) (Bond distances in Angstroms and angles in degrees)
7-8	**Table S2** Zero point energy (ZPE(298K)/(kcal·mol^{-1})), relative energies (ΔE(298K) and $\Delta(E$ + ZPE)(298K)/(kcal·mol^{-1})), enthalpies (ΔH(298K)/(kcal·mol^{-1})), entropy (S/(cal·mol^{-1}·K^{-1})) and free energies (ΔG(298K)/(kcal·mol^{-1})) for the reactant complexes of $CH_2OO\cdots(H_2O)_n$ (n = 1-4)[a]
9	**Table S3** Zero point energy (ZPE(298K)/(kcal·mol^{-1})), relative energies (ΔE(298K) and $\Delta(E$ + ZPE)(298K)/(kcal·mol^{-1})), enthalpies (ΔH(298K)/(kcal·mol^{-1})), entropy (S/(cal·mol^{-1}·K^{-1})), and free energies (ΔG(298K)/(kcal·mol^{-1})) for the favorable routes of the CH_2OO + $(H_2O)_n$ (n = 1-4) reaction[a]
10	**Fig. S4** Schematic energy diagrams for the unfavorable routes of the CH_2OO + $(H_2O)_2$ reaction at the CCSD(T)-F12a/cc-pVDZ-F12//B3LYP/6-311+G(2*d*,2*p*) level
11	**Fig. S5** Schematic energy diagrams for the unfavorable routes of the CH_2OO + $(H_2O)_3$ reaction at the CCSD(T)-F12a/cc-pVDZ-F12//B3LYP/6-311+G(2*d*,2*p*) level

* Corresponding authors. Tel: +86-0916-2641083, Fax: +86-0916-2641083.
E-mail:ztianlei88@163.com(T.L. Zhang);wangzq128@163.com(Z.Q. Wang).
# These authors are contributed equally to this work.
† Electronic supplementary information (ESI) available.

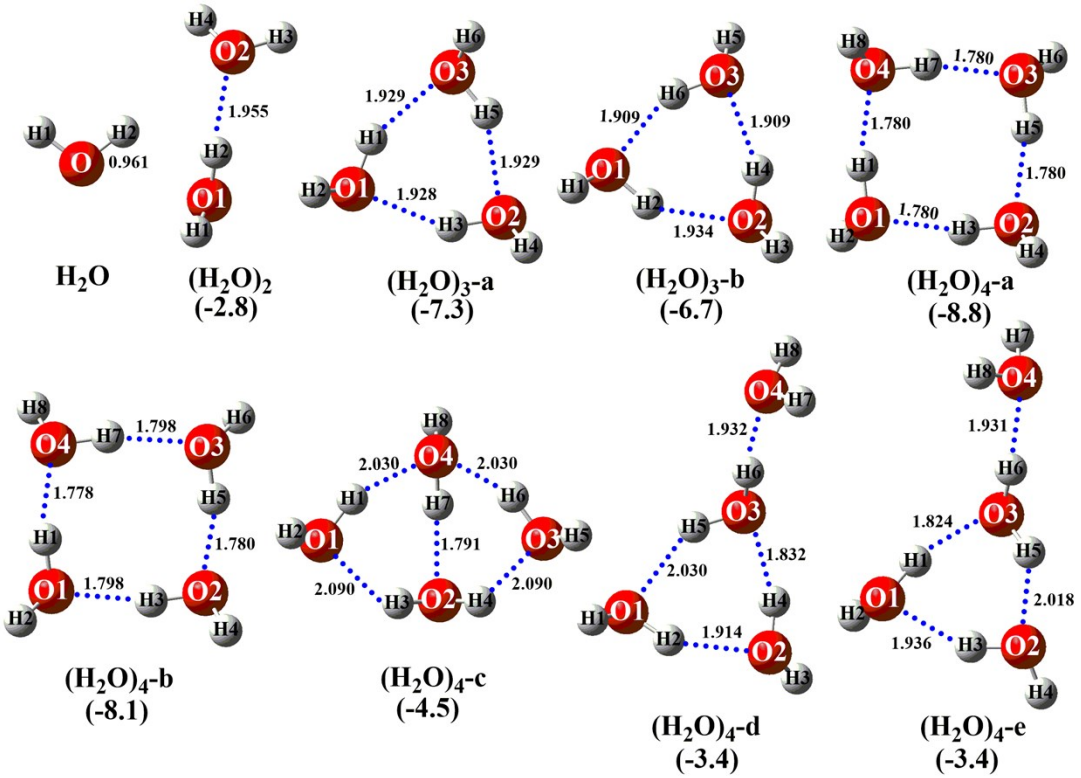

Fig. S1 Optimized geometries and the binding energy for the complexes of $(H_2O)_n$ (n = 1-4) at the CCSD(T)-F12a/cc-pVDZ-F12//B3LYP/6-311+G(2*d*,2*p*) level of theory (in kcal·mol^{-1}) (Bond distances in Angstroms and angles in degrees)

Table S1 Zero point energies (ZPE/(kcal·mol^{-1})), relative energies (ΔE and $\Delta(E$+ZPE)/ (kcal·mol^{-1})), enthalpies (ΔH(298K)/(kcal·mol^{-1})), entropy (S(298)/(cal·mol^{-1}·K^{-1})), and free energies (ΔG(298K)/(kcal·mol^{-1})) for the $(H_2O)_n$ (n = 2-4)[a]

Species	ZPE	ΔE	ΔG	S	$\Delta(E$ + ZPE)	ΔH
$H_2O + H_2O$	26.8	0.0	0.0	90.2	0.0	0.0
$(H_2O)_2$	29.1	-5.0 (-5.0)[b]	2.9 (2.6)[b]	69.2	-2.8 (-2.9)[b]	-3.3 (-3.3)[b]
$H_2O + (H_2O)_2$	42.5	0.0	0.0	114.3	0.0	0.0
$(H_2O)_3$-a	45.8	-10.6 (-10.9)[b]	1.8 (1.3)[b]	79.3	-7.3 (-7.6)[b]	-8.6 (-8.8)[b]
$(H_2O)_3$-b	45.6	-9.8 (-10.1)[b]	2.2 (1.2)[b]	80.4	-6.7 (-7.2)[b]	-7.9 (-8.1)[b]
$H_2O + (H_2O)_3$	59.3	0.0	0.0	124.4	0.0	0.0
$(H_2O)_2 + (H_2O)_2$	58.1	5.6 (5.8)[b]	1.1 (0.1)[b]	138.5	4.5 (4.1)[b]	5.3 (5.17)[b]
$(H_2O)_4$-a	62.1	-11.7 (-11.7)[b]	-0.1 (-0.4)[b]	91.9	-8.8 (-8.8)[b]	-9.8 (-9.7)[b]
$(H_2O)_4$-b	61.9	-10.8 (-10.8)[b]	0.4 (0.2)[b]	93.0	-8.1 (-8.1)[b]	-9.0 (-8.9)[b]
$(H_2O)_4$-c	61.5	-6.7	3.5	95.8	-4.5	-5.0
$(H_2O)_4$-d	61.0	-5.2 (-5.2)[b]	3.3 (2.9)[b]	101.5	-3.4 (-3.3)[b]	-3.5 (-3.4)[b]
$(H_2O)_4$-e	60.9	-5.1	2.8	103.5	-3.4	-3.5

[a] ZPE and S values obtained at B3LYP/6-311+G(2*d*,2*p*) level of theory; The energy values are obtained at CCSD(T)-F12a/cc-pVDZ-F12//B3LYP/6-311+G(2*d*,2*p*) level whereas the *H* and *G* corrections are taken from the B3LYP/6-311+G(2*d*,2*p*) level;

[b] The values in parentheses are the previously report from reference (*J. Phys. Chem. A*, 2013, 117, 10381-10396.) .

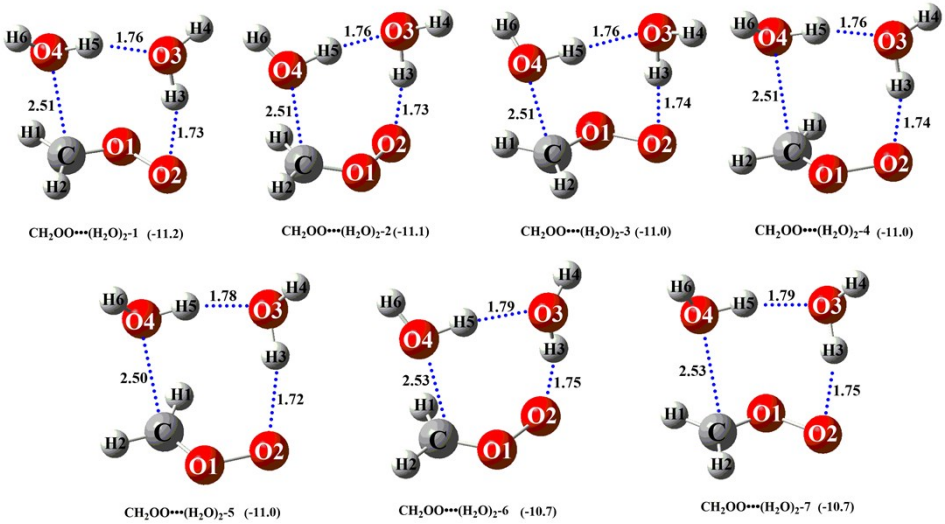

Fig. S2 The most stable geometry and the binding energy of $CH_2OO\cdots(H_2O)_2$ complexes searched by ABCluster program (in kcal·mol^{-1}) (Bond distances in Angstroms and angles in degrees)

In order to verify the accuracy of the stable complexes searched by the TGMin program, the similar cluster searching program named ABCluster program [1,2] has been adopted to verify the stable complexes again. The calculated results show that the obtained stable complexes by ABCluster program is highly agreeable consistent with our results (Fig. S2). So, global minimum searching using Tsinghua Global Minimum program has been introduced to find the most stable geometry of $CH_2OO\cdots (H_2O)_n$ (n = 1-4) complex in the present work.

Reference

1. J. Zhang and M. Dolg, *Phys. Chem. Chem. Phys*. 2016, **18**, 3003-3010.

2. J. Zhang and M. Dolg, *Phys. Chem. Chem. Phys*. 2015, **17**, 24173-24181.

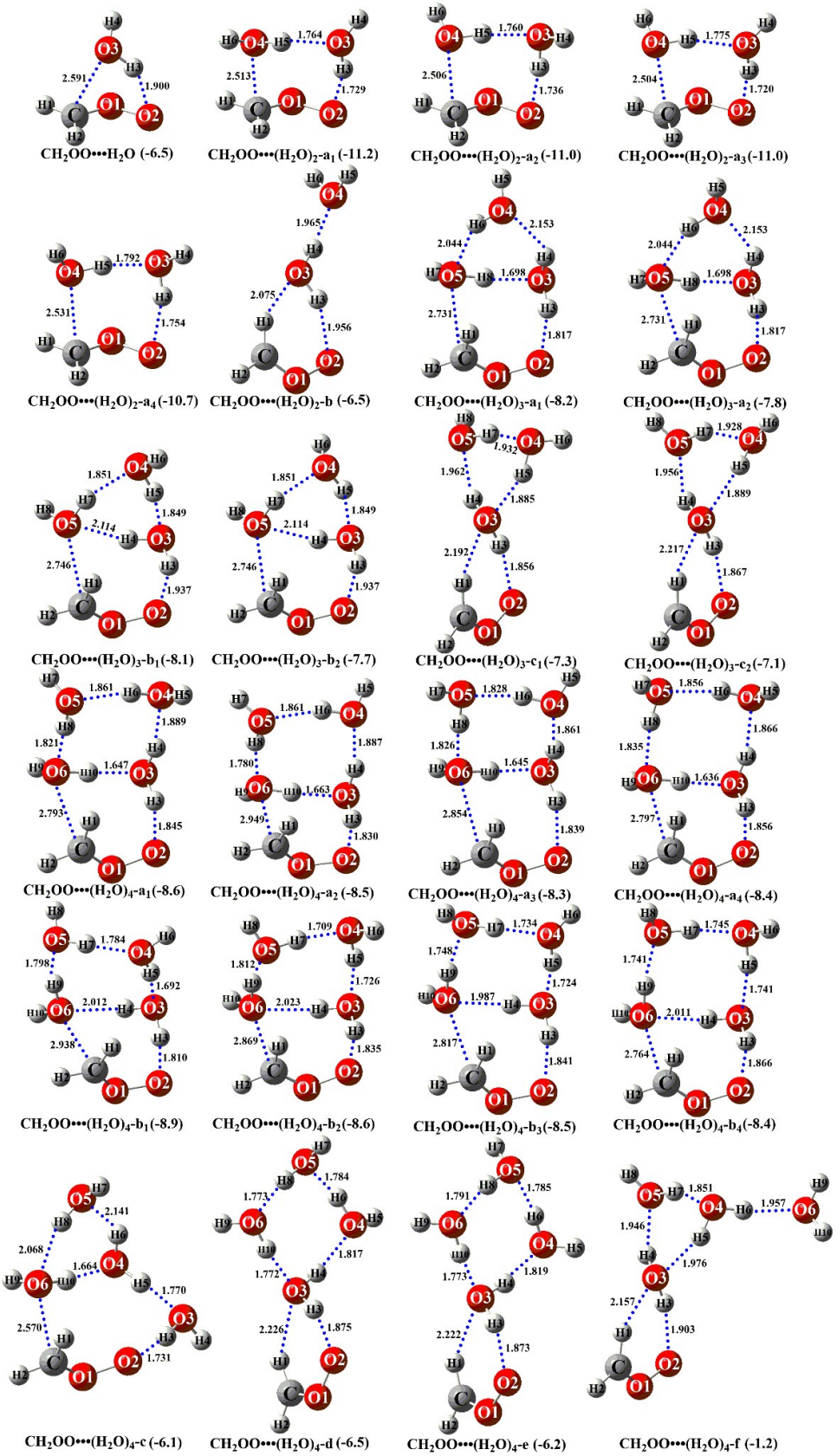

Fig. S3 The geometrical possible structures and the binding energy for the $CH_2OO\cdots(H_2O)_n$ (n = 1-4) complexes at the CCSD(T)-F12a/cc-pVDZ-F12//B3LYP/6-311+G(2*d*,2*p*) level of theory (in kcal·mol^{-1}) (Bond distances in Angstroms and angles in degrees)

Table S2 Zero point energy (ZPE(298K)/(kcal·mol^{-1})), relative energies (ΔE(298K) and $\Delta(E$ + ZPE)(298K)/(kcal·mol^{-1})), enthalpies (ΔH(298K)/(kcal·mol^{-1})), entropy (S/(cal·mol^{-1}·K^{-1})) and free energies (ΔG(298K)/(kcal·mol^{-1})) for the reactant complexes of $CH_2OO\cdots(H_2O)_n$ (n = 1-4)[a]

Species	ZPE	ΔE	ΔG	S	$\Delta(E$ + ZPE)	ΔH
$CH_2OO + H_2O$	33.0	0.0	0.0	104.6	0.0	0.0
$CH_2OO\cdots H_2O$	35.0	-8.6	0.9	78.1	-6.5	-7.0
$CH_2OO + (H_2O)_2$	48.6	0.0	0.0	128.8	0.0	0.0
$CH_2OO\cdots(H_2O)_2$-a_1	51.3	-13.9	-0.1	88.2	-11.2	-12.2
$CH_2OO\cdots(H_2O)_2$-a_2	51.3	-13.7	0.0	88.5	-11.0	-12.0
$CH_2OO\cdots(H_2O)_2$-a_3	51.2	-13.6	0.0	89.1	-11.0	-11.9
$CH_2OO\cdots(H_2O)_2$-a_4	51.0	-13.2	0.1	89.7	-10.7	-11.5
$CH_2OO\cdots(H_2O)_2$-b	50.1	-8.0	1.4	102.8	-6.5	-6.4
$CH_2OO + (H_2O)_3$	65.1	0.0	0.0	140.0	0.0	0.0
$CH_2OO\cdots(H_2O)_3$-a_1	67.2	-10.2	2.5	102.6	-8.2	-8.6
$CH_2OO\cdots(H_2O)_3$-a_2	67.1	-9.8	2.9	102.7	-7.8	-8.2
$CH_2OO\cdots(H_2O)_3$-b_1	66.9	-9.9	1.9	106.0	-8.1	-8.2
$CH_2OO\cdots(H_2O)_3$-b_2	67.0	-9.5	2.2	106.1	-7.7	-7.8
$CH_2OO\cdots(H_2O)_3$-c_1	66.8	-9.0	1.6	110.0	-7.3	-7.3
$CH_2OO\cdots(H_2O)_3$-c_2	66.8	-8.8	2.0	109.7	-7.1	-7.1
$CH_2OO + (H_2O)_4$	81.6	0.0	0.0	151.5	0.0	0.0
$CH_2OO\cdots(H_2O)_4$-a_1	82.9	-9.9	0.8	120.5	-8.6	-8.4
$CH_2OO\cdots(H_2O)_4$-a_2	82.8	-9.7	1.2	119.8	-8.5	-8.3
$CH_2OO\cdots(H_2O)_4$-a_3	83.0	-9.7	1.4	119.2	-8.3	-8.3
$CH_2OO\cdots(H_2O)_4$-a_4	82.8	-9.5	0.9	121.3	-8.4	-8.1
$CH_2OO\cdots(H_2O)_4$-b_1	83.0	-10.3	1.5	116.9	-8.9	-8.8
$CH_2OO\cdots(H_2O)_4$-b_2	83.0	-10.0	1.6	117.4	-8.6	-8.6
$CH_2OO\cdots(H_2O)_4$-b_3	82.9	-9.7	1.1	119.7	-8.5	-8.3
$CH_2OO\cdots(H_2O)_4$-b_4	82.8	-9.6	1.1	120.5	-8.4	-8.2
$CH_2OO\cdots(H_2O)_4$-c	82.8	-7.3	3.7	119.4	-6.1	-5.9
$CH_2OO\cdots(H_2O)_4$-d	83.0	-7.9	2.4	122.5	-6.5	-6.3
$CH_2OO\cdots(H_2O)_4$-e	82.9	-7.5	2.5	123.3	-6.2	-5.9
$CH_2OO\cdots(H_2O)_4$-f	81.9	-1.5	6.3	128.1	-1.2	-0.7

[a] ZPE and S values obtained at B3LYP/6-311+G(2*d*,2*p*) level of theory; The energy values are obtained at CCSD(T)-F12a/cc-pVDZ-F12//B3LYP/6-311+G(2*d*,2*p*) level whereas the *H* and *G* corrections are taken from the B3LYP/6-311+G(2*d*,2*p*) level

Though some isomers shown in Table S2 have positive Gibbs free energy of formation, and thus would not form spontaneously owing to the large entropic penalty.[1,2] However, as seen in references,[3-14] water catalyzed reactions starting from hydrogen bonded complexes between water and reactant remains a major route to estimate the catalytic effect of water on atmospheric reaction in tropospheric conditions.

Reference:

1. S. S. Iyengar, *J. Chem. Phys.*, 2005, **123**, 084310.

2. S. M. Dietrick, A. B. Pacheco, P. Phatak, P. S. Stevens and S. S. Iyengar, *J. Phys. Chem. A*, 2012, **116**, 399-414.
3. W. Chao, J. T. Hsieh and C. H. Chang, *Science*, 2015, **347**, 751-754.
4. C. Zhu, M. Kumar, J. Zhong, L. Li, J. S. Francisco and X. C. Zeng, *J. Am. Chem. Soc.*, 2016, **138**, 11164-11169.
5. T. Berndt, J. Voigtländer, F. Stratmann, H. Junninen, R. L. Mauldin III, M. Sipilä, M. Kulmalab and H. Herrmanna, *Phys. Chem. Chem. Phys.*, 2014, **16**, 19130-19136.
6. T. R. Lewis, M. A. Blitz, D. E. Heard and W. Seakins, *Phys. Chem. Chem. Phys.*, 2015, **17**, 4859-4863.
7. L. C. Lin, H. T. Chang, C. H. Chang, W. Chao, M. C. Smith, C. H. Chang, J. J. M. Lin and K. Takahashi, *Phys. Chem. Chem. Phys.*, 2016, **18**, 4557-4568.
8. X. F. Tan, B. Long, D. S. Ren, W. J. Zhang, Z. W. Long and E. Mitchell, *Phys. Chem. Chem. Phys.*, 2018, **20**, 7701-7709.
9. M. C. Smith, C. H. Chang, W. Chao, L. C. Lin, K. Takahashi, K. A. Boering and J. J. M. Lin, *J. Phys. Chem. Lett.*, 2015, **6**, 2708-2713.
10. M. K. Louie, J. S. Francisco, M. Verdicchio, S. J. Klippenstein and A. Sinha, *J. Phys. Chem. A*, 2016, **120**, 1358-1368.
11. B. Bandyopadhyay, P. Kumar and P. Biswas, *J. Phys. Chem. A*, 2017, **121**, 3101-3108.
12. S. Mallick, S. Sarkar, B. Bandyopadhyay and P. Kumar, *J. Phys. Chem. A*, 2018, **122**, 350-363.
13. L. Chen, W. Wang, L. Zhou, W. Wang, F. Liu, C. Li and J. Lü. *Theor. Chem. Acc.*, 2016, **135**, 252.
14. L. Chen, W. Wang, W. Wang, Y. Liu, F. Liu, N. Liu and B. Wang, *Theor. Chem. Acc.*, 2016, **135**, 131.

Table S3 Zero point energy (ZPE(298K)/(kcal·mol^{-1})), relative energies (ΔE(298K) and $\Delta(E$ + ZPE)(298K)/(kcal·mol^{-1})), enthalpies (ΔH(298K)/(kcal·mol^{-1})), entropy (S/(cal·mol^{-1}·K^{-1})), and free energies (ΔG(298K)/(kcal·mol^{-1})) for the favorable routes of the $CH_2OO + (H_2O)_n$ (n = 1-4) reaction[a]

Species	ZPE	ΔE	ΔG	S	$\Delta(E$ + ZPE)	ΔH
$CH_2OO + H_2O$	33.0	0.0	0.0	104.6	0.0	0.0
$CH_2OO\cdots H_2O$	35.4	-7.5	3.4	74.0	-5.0	-5.7
TS_WM	35.4	0.0	12.1	66.5	2.5	0.7
$HOCH_2OOH$	38.0	-47.7	-33.5	69.2	-42.7	-44.1
$CH_2OO + (H_2O)_2$	48.6	0.0	0.0	128.8	0.0	0.0
$CH_2OO\cdots(H_2O)_2$-a_1	51.3	-13.9	-0.1	88.2	-11.2	-12.2
TS_WD1a_1	51.1	-9.5	5.9	77.3	-7.0	-9.4
IMF_WD1a_1	54.0	-51.3	-33.7	82.6	-45.9	-47.5
$HOCH_2OOH + H_2O$	51.4	-42.7	-36.4	114.2	-39.9	-40.7
$CH_2OO + (H_2O)_3$	65.1	0.0	0.0	140.0	0.0	0.0
$CH_2OO\cdots(H_2O)_3$-a_1	67.2	-10.2	2.5	102.6	-8.2	-8.6
TS_WT1a_1	65.5	-3.9	8.0	96.8	-3.5	-4.9
IMF_WT1a_1	69.8	-51.0	-34.8	97.9	-46.3	-47.3
$CH_2OO\cdots(H_2O)_3$-b_1	66.9	-9.9	1.9	106.0	-8.1	-8.2
TS_WT2b_1	65.8	-6.5	4.0	106.6	-5.8	-5.9
IM_WT3b_1	67.0	-13.2	-1.0	104.0	-11.4	-11.8
TS_WT3b_1	66.5	-8.4	5.8	90.2	-7.0	-9.1
IMF_WT3b_1	69.8	-51.0	-34.8	97.9	-46.3	-47.3
$HOCH_2OOH + (H_2O)_2$	67.0	-37.8	-35.7	138.4	-36.0	-36.1
$CH_2OO + (H_2O)_4$	81.6	0.0	0.0	151.5	0.0	0.0
$CH_2OO\cdots(H_2O)_4$-a_1	82.9	-9.9	0.8	120.5	-8.6	-8.4
TS_WQ1a_1	81.6	-2.4	9.6	106.9	-2.4	-3.7
IMF_WQ1a_1	85.4	-47.1	-32.8	114.8	-43.4	-43.8
$CH_2OO\cdots(H_2O)_4$-b_1	83.0	-10.3	1.5	116.9	-8.9	-8.8
TS_WQ2b_1	82.5	1.6	13.2	113.1	2.5	1.8
IM_WQ3b_1	82.6	-9.1	1.1	121.2	-8.2	-7.9
TS_WQ3b_1	79.2	6.2	16.5	100.7	3.7	1.4
IMF_WQ3b_1	85.8	-49.0	-33.5	110.8	-44.9	-45.6
$HOCH_2OOH + (H_2O)_3$	83.6	-35.2	-33.0	149.6	-33.3	-33.6

[a] ZPE and S values obtained at B3LYP/6-311+G(2*d*,2*p*) level of theory; The energy values are obtained at the CCSD(T)-F12a/cc-pVDZ-F12//B3LYP/6-311+G(2*d*,2*p*) level whereas the *H* and *G* corrections are taken from the B3LYP/6-311+G(2*d*,2*p*) level

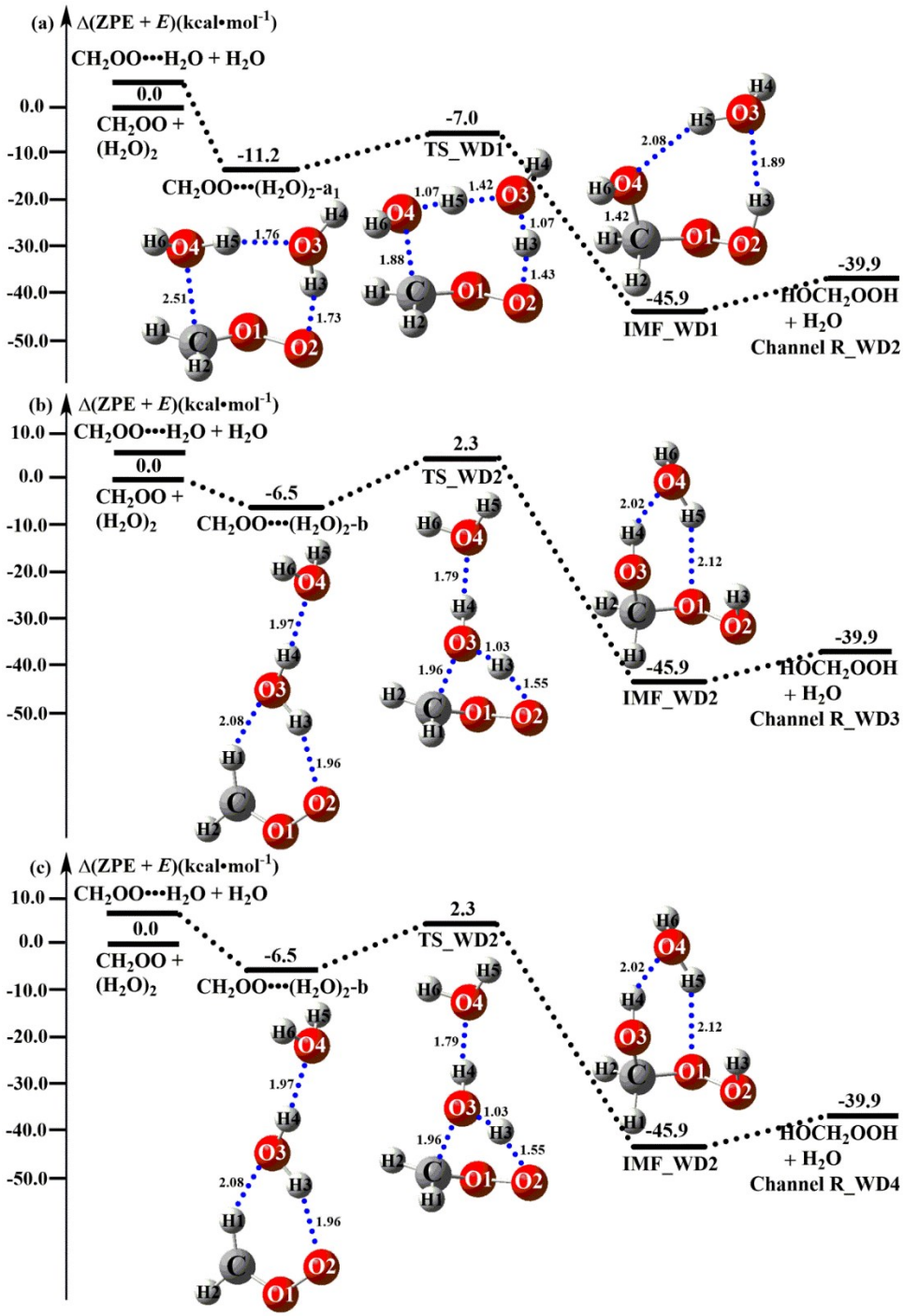

Fig. S4 Schematic energy diagrams for the unfavorable routes of the $CH_2OO + (H_2O)_2$ reaction at the CCSD(T)-F12a/cc-pVDZ-F12//B3LYP/6-311+G(2*d*,2*p*) level

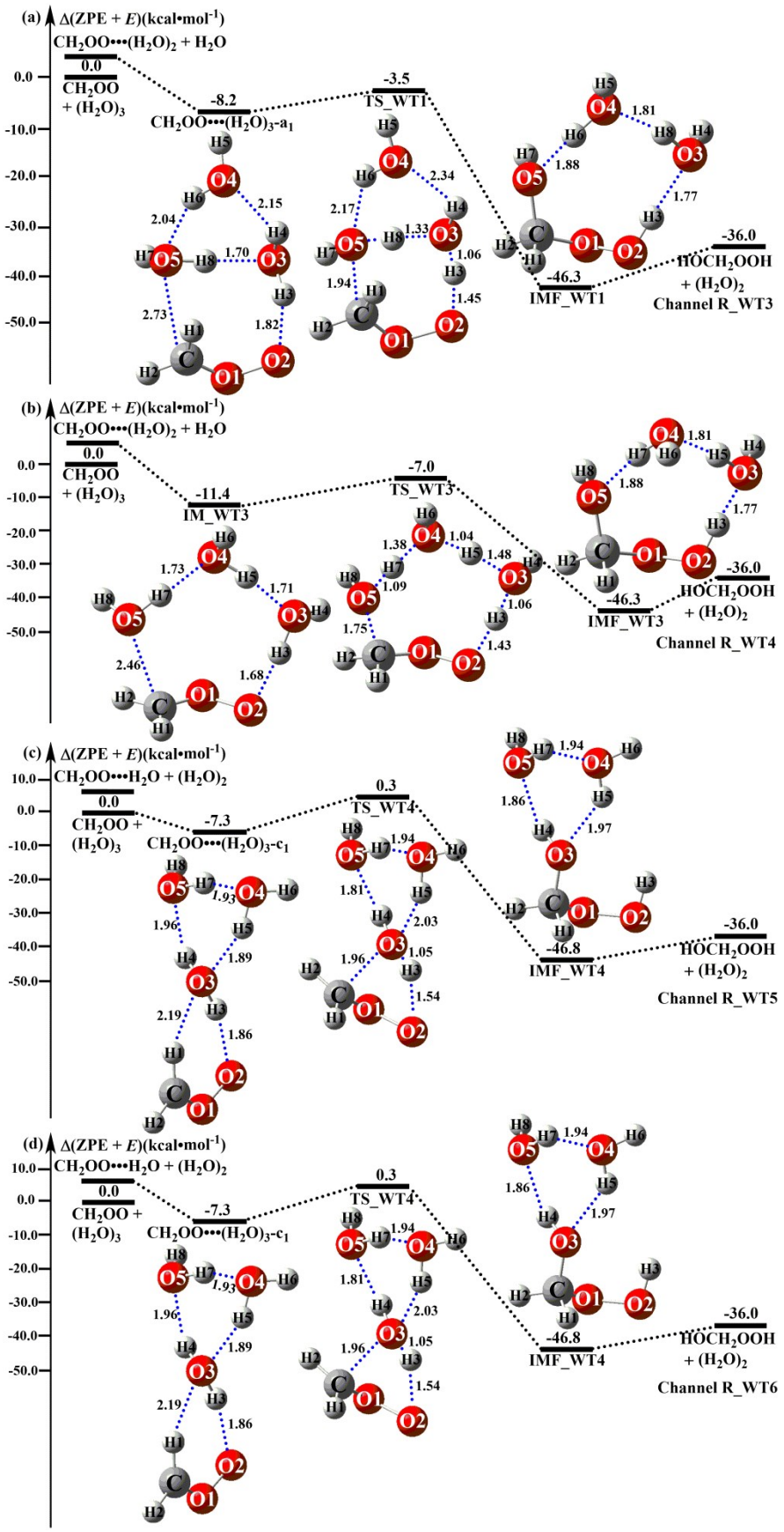

Fig. S5 Schematic energy diagrams for the unfavorable routes of the $CH_2OO + (H_2O)_3$ reaction at the CCSD(T)-F12a/cc-pVDZ-F12//B3LYP/6-311+G(2*d*,2*p*) level

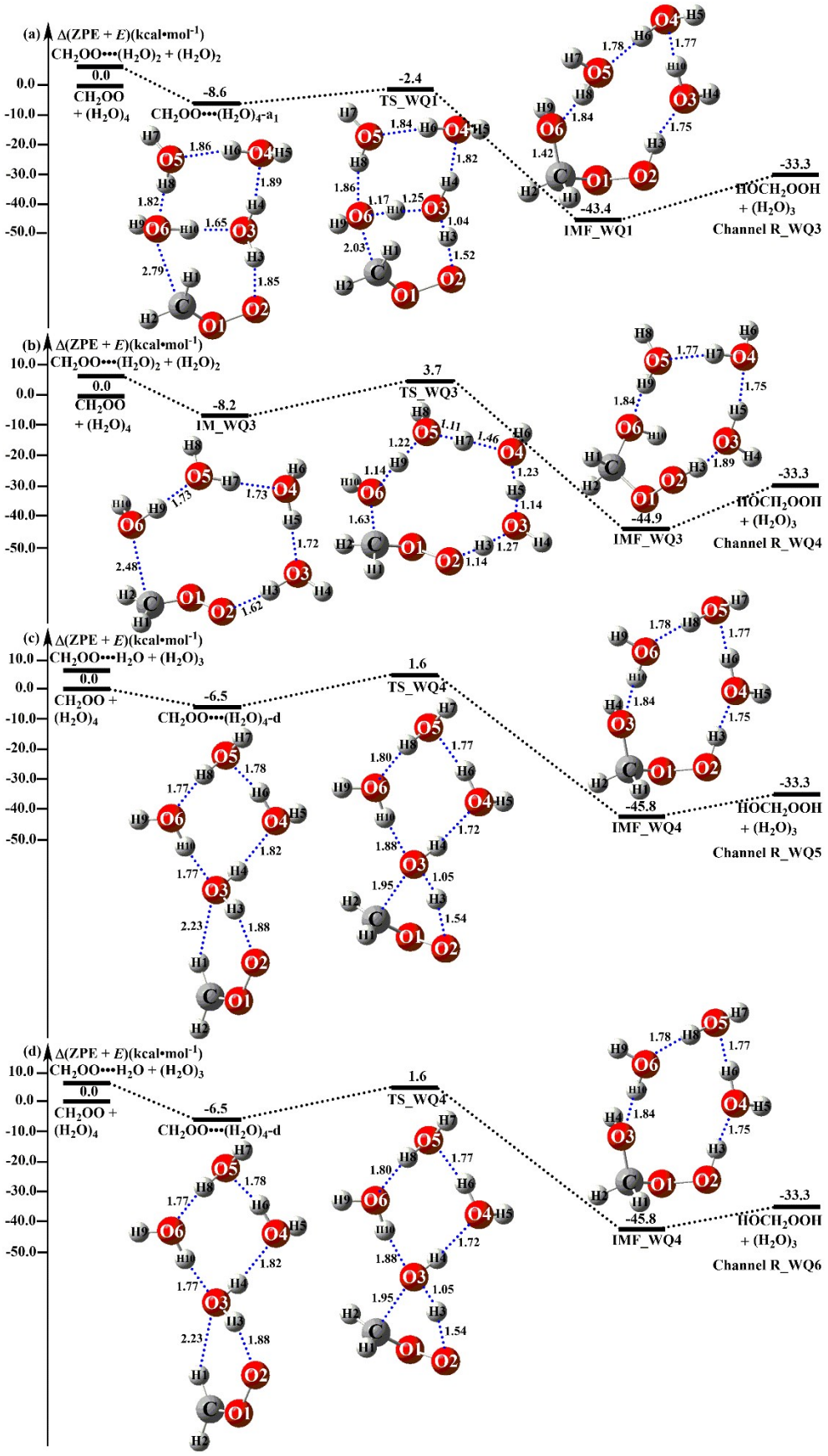

Fig. S6 Schematic energy diagrams for the unfavorable routes of the $CH_2OO + (H_2O)_4$ reaction at the CCSD(T)-F12a/cc-pVDZ-F12//B3LYP/6-311+G(2*d*,2*p*) level

Born-Oppenheimer molecular dynamics simulations

To examined the reaction between CH_2OO and $(H_2O)_n$ (n = 1-3) at the gas phase using the BOMD simulations based on the DFT method employed in the CP2K[1] program package. The atomic forces were calculated within the DFT framework using the BOMD simulation. To avoid the effects of initial configurations, we only choose the $CH_2OO\cdots(H_2O)_n$ (n = 1-3) complex with the largest concentration and stabilizing energy were produced by the TGmin program. A cubic simulation box of side 35 Å was used. The resulting box size was found to be large enough to eliminate any interaction between the adjacent periodic images. The system was fully relaxed using a DFT method preceding the BOMD simulations, where the exchange and correlation interaction is treated with the Becke-Lee-Yang-Parr (BLYP)[2,3] functional. To account for the weak dispersion interactions (BLYP-D3), the Grimme's dispersion correction method[4,5] was applied. The valence and the core electrons were treated by a double-ζ Gaussian basis set combined with an auxiliary basis set[6] and the Goedecker-Teter-Hutter (GTH) norm-conserved pseudopotentials.[7] For the plane-wave basis set, an energy cutoff of 280 Rydberg was used while a 40 Rydberg cutoff was used for the Gaussian basis set. The BOMD (BLYP-D3) simulation was performed in the constant volume and temperature ensemble (NVT) and the constant energy and volume ensemble (NVE), accompanied by the Nose-Hoover chain method for controlling the temperature (300 K) of the system. The integration step is set as 1 fs, which has been previously shown to attain sufficient energy conservation for the water system.[8-13]

Reference

1. J. VandeVondele, M. Krack, F. Mohamed, M. Parrinello, T. Chassaing and J. Hutter, *Comput. Phys. Commun.*, 2005, **167**, 103-128.
2. D. Becke, *Phys. Rev. A*, 1988, **38**, 3098.
3. T. Lee, W. T. Yang and R. G. Parr, *Phys. Rev. B*, 1988, **37**, 785.
4. S. Grimme, *J. Comput. Chem.*, 2004, **25**, 1463-1473.
5. S. Grimme, *J. Comput. Chem.*, 2006, **27**, 1787-1799.
6. S. Goedecker, M. Teter and J. Hutter, *Phys. Rev. B*, 1996, **54**, 1703.
7. C. Hartwigsen, S. Goedecker and J. Hutter, *Phys. Rev. B*, 1998,**58**, 3641
8. J. Zhong, M. Kumar, J. S. Francisco and X. C. Zeng, *Acc. Chem. Res.*, 2018, **51**, 1229-1237.
9. C. Zhu, M. Kumar, J. Zhong, L. Li, J. S. Francisco and X. C. Zeng, *J. Am. Chem. Soc.*, 2016, **138**, 11164-11169.
10. L. Li, M. Kumar, C. Q. Zhu, J. Zhong, J. S. Francisco and X. C. Zeng, *J. Am. Chem. Soc.*, 2016, **138**, 1816-1819.
11. J. Zhong, M. Kumar, C. Q. Zhu, J. S. Francisco and X. C. Zeng, *Angew. Chem., Int. Ed.*, 2017, **56**, 7740-7744.
12. M. Kumar, J. Zhong, X. C. Zeng and J. S. Francisco, *Chem. Sci.*, 2017, **8**, 5385-5391.
13. M. Kumar, J. Zhong, X. C. Zeng and J. S. Francisco, *J. Am. Chem. Soc.*, 2018, **140**, 4913-4921.

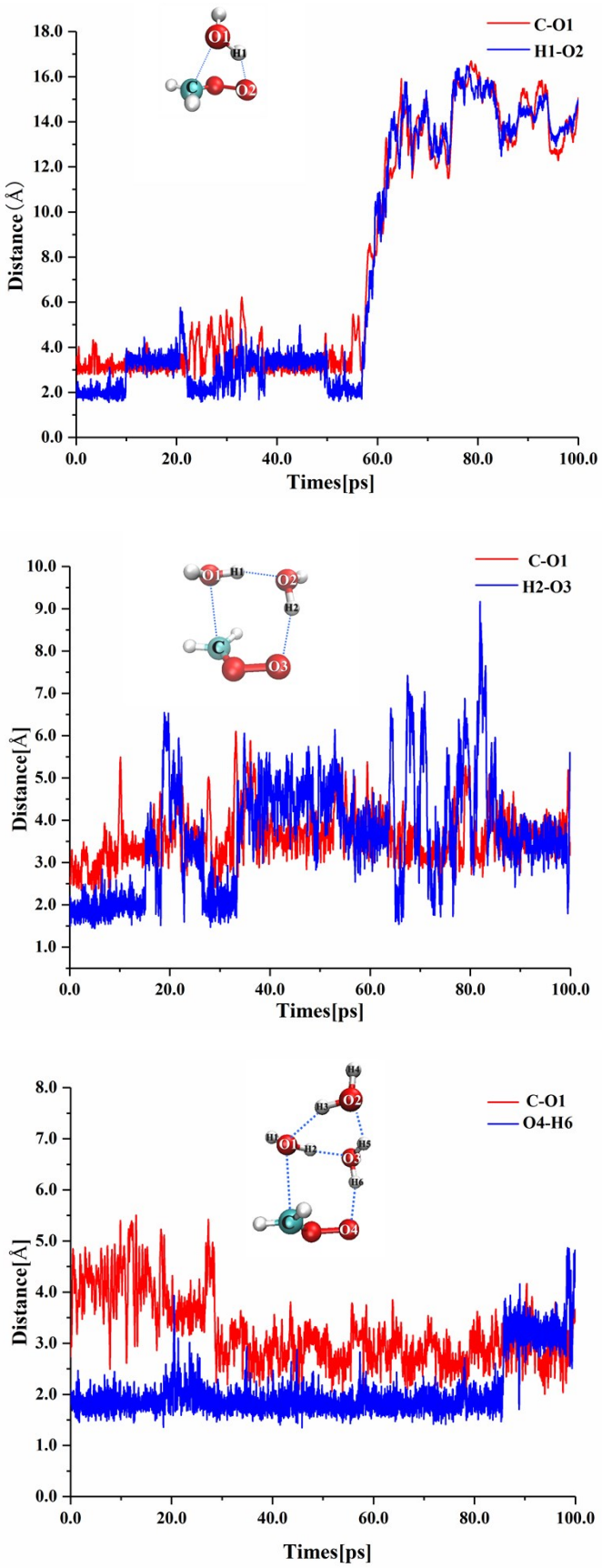

Fig. S7 The trajectories of BOMD simulation combined with NVT ensemble for the the favorable channels of the gas phase hydrolysis reaction of CH_2OO with $(H_2O)_n$ (n = 1-3)

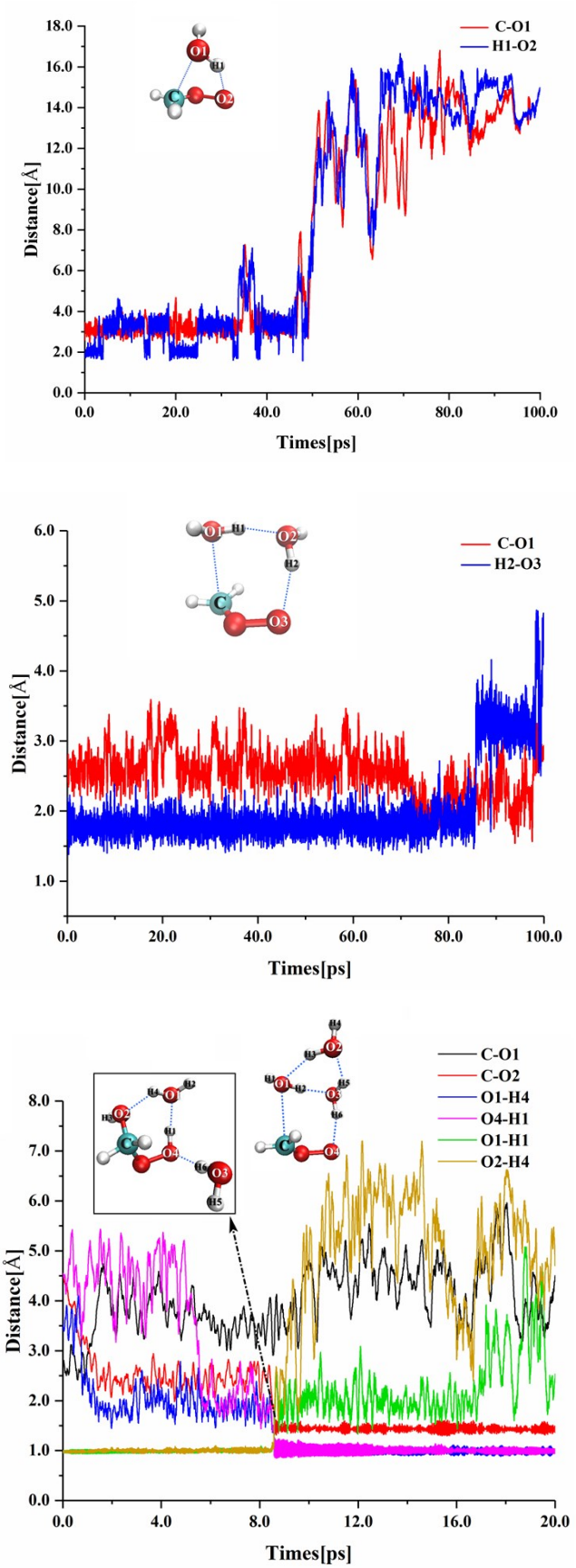

Fig. S8 The trajectories of BOMD simulation combined with NVE ensemble for the the favorable channels of the gas phase hydrolysis reaction of CH_2OO with $(H_2O)_n$ (n = 1-3)

Above BOMD simulations results of the NVE simulation results show that the CH_2OO + H_2O and CH_2OO + $(H_2O)_2$ reactions will not occur within the time scale of 100 ps. However, the NVE simulation results show that the CH_2OO + $(H_2O)_3$ reaction can be completed at 7.0 ps. This difference may be due to the additional water molecules increasing the stability of CH_2OO in the atmosphere. These results probably support that the gas phase reaction of CH_2OO + $(H_2O)_3$ reaction is not negligible in the atmosphere. Besides, the results of the NVT simulation show that all the favorable channels involved in the reaction of CH_2OO and $(H_2O)_n$ (n = 1-3) cannot react on a time scale of 100 ps. This is slower by 2-3 orders of magnitude than that at the air/water interface reported by Zhu *et al*.[39,] indicating that the gas phase reaction of CH_2OO with $(H_2O)_n$ (n = 1-3) may be harder to occur as compared with its hydrolysis at the air/water interface.

1. C. Zhu, M. Kumar, J. Zhong, L. Li, J. S. Francisco and X. C. Zeng, *J. Am. Chem. Soc.*, 2016, **138**, 11164-11169.

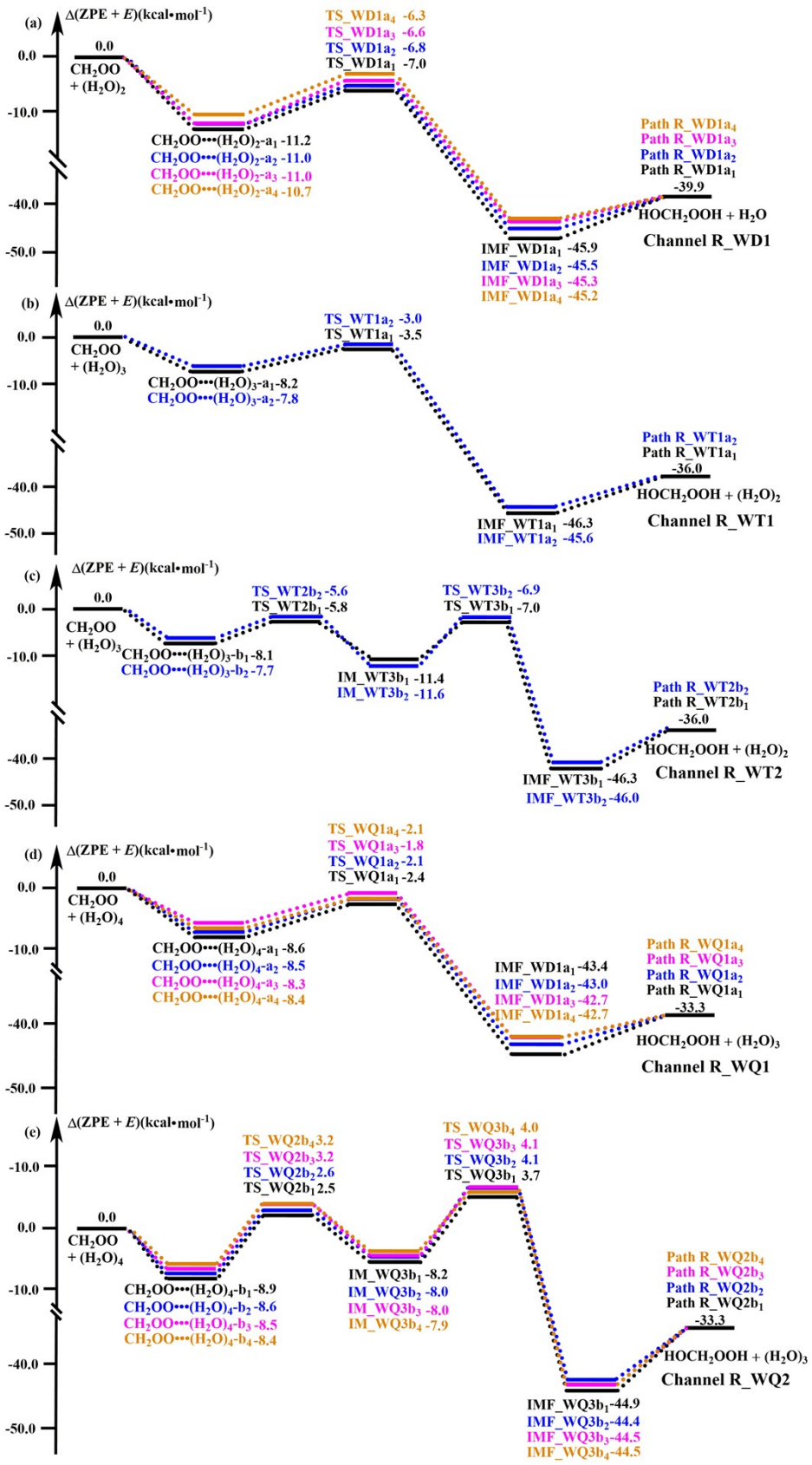

Fig. S9 Schematic energy diagrams for the favorable channels of the $CH_2OO + (H_2O)_n$ (n = 2-4) reactions starting from geometric isomers of $CH_2OO\cdots(H_2O)_n$ (n = 2-4) complexes at the CCSD(T)-F12a/cc-pVDZ-F12//B3LYP/6-311+G(2*d*,2*p*) level

Table S4 Rate constants ($cm^3 \cdot molecules^{-1} \cdot s^{-1}$) for the $CH_2OO + (H_2O)_n$ (n = 1-4) reaction within the temperature range of 290-320 K

Catalyst	Rate Constant.	Temperature(K)				
		290	298	300	310	320
Channel R_WM1	K_{eq}	7.94E-21	5.84E-21	5.42E-21	3.80E-21	2.72E-21
	k_{uni}	2.82E+04	4.14E+04	4.54E+04	7.08E+04	1.07E+05
	k_b	2.24E-16	2.42E-16	2.46E-16	2.69E-16	2.92E-16
Path R_WD1a$_1$	K_{eq}	3.11E-20	2.02E-20	1.82E-20	1.11E-20	6.95E-21
	k_{uni}	3.21E+08	3.69E+08	3.81E+08	4.47E+08	5.19E+08
	k_b	9.96E-12	7.45E-12	6.94E-12	4.95E-12	3.61E-12
Channel R_WD2	K_{eq}	1.78E-21	1.25E-21	1.15E-21	7.65E-22	5.23E-22
	k_{uni}	3.21E+08	3.69E+08	3.81E+08	4.47E+08	5.19E+08
	k_b	5.69E-13	4.61E-13	4.38E-13	3.42E-13	2.72E-13
Channel R_WD3	K_{eq}	9.18E-22	7.74E-22	7.43E-22	6.12E-22	5.12E-22
	k_{uni}	6.76E+03	9.51E+03	1.03E+04	1.53E+04	2.21E+04
	k_b	6.21E-18	7.36E-18	7.67E-18	9.36E-18	1.13E-17
Channel R_WD4	K_{eq}	5.25E-23	4.79E-23	4.69E-23	4.23E-23	3.85E-23
	k_{uni}	6.76E+03	9.51E+03	1.03E+04	1.53E+04	2.21E+04
	k_b	3.55E-19	4.56E-19	4.84E-19	6.47E-19	8.51E-19
Path R_WT1a$_1$	K_{eq}	4.25E-21	2.92E-21	2.67E-21	1.73E-21	1.15E-21
	k_{uni}	7.82E+08	9.42E+08	9.85E+08	1.22E+09	1.49E+09
	k_b	3.33E-12	2.75E-12	2.63E-12	2.11E-12	1.72E-12
Path R_WT2b$_1$	K_{eq}	1.17E-20	8.22E-21	7.54E-21	5.00E-21	3.40E-21
	k_{uni}[a]	6.57E+07	7.60E+07	7.88E+07	9.31E+07	1.09E+08
	k_b	7.71E-13	6.25E-13	5.94E-13	4.65E-13	3.70E-13
Channel R_WT3	K_{eq}	4.50E-23	3.74E-23	3.58E-23	2.89E-23	2.37E-23
	k_{uni}	7.82E+08	9.42E+08	9.85E+08	1.22E+09	1.49E+09
	k_b	3.52E-14	3.52E-14	3.52E-14	3.53E-14	3.53E-14
Channel	K_{eq}	2.13E-20	1.53E-20	1.41E-20	9.65E-21	6.75E-21

	k_{uni}	6.57E+07	7.61E+07	7.88E+07	9.32E+07	1.09E+08
	k_b	1.40E-12	1.17E-12	1.11E-12	8.99E-13	7.34E-13
Channel R_WT5	K_{eq}	1.81E-20	1.32E-20	1.22E-20	8.51E-21	6.07E-21
	k_{uni}	5.22E+05	7.24E+05	7.83E+05	1.14E+06	1.63E+06
	k_b	9.43E-15	9.55E-15	9.58E-15	9.73E-15	9.88E-15
Channel R_WT6	K_{eq}	7.48E-23	5.85E-23	5.51E-23	4.14E-23	3.18E-23
	k_{uni}	5.22E+05	7.24E+05	7.83E+05	1.14E+06	1.63E+06
	k_b	3.91E-17	4.23E-17	4.31E-17	4.74E-17	5.18E-17
Path R_WQ1a$_1$	K_{eq}	5.35E-21	4.09E-21	3.83E-21	2.81E-21	2.11E-21
	k_{uni}	2.87E+07	3.38E+07	3.52E+07	4.25E+07	5.08E+07
	k_b	1.54E-13	1.38E-13	1.35E-13	1.20E-13	1.07E-13
Path R_WQ2b$_1$	K_{eq}	1.71E-20	1.25E-20	1.16E-20	8.12E-21	5.82E-21
	k_{uni}	6.41E+01	9.54E+01	1.05E+02	1.67E+02	2.57E+02
	k_b	1.10E-18	1.19E-18	1.22E-18	1.35E-18	1.50E-18
Channel R_WQ3	K_{eq}	6.60E-21	4.67E-21	4.29E-21	2.87E-21	1.98E-21
	k_{uni}	2.87E+07	3.38E+07	3.52E+07	4.25E+07	5.08E+07
	k_b	1.89E-13	1.58E-13	1.51E-13	1.22E-13	1.00E-13
Channel R_WQ4	K_{eq}	3.67E-20	2.50E-20	2.28E-20	1.46E-20	9.64E-21
	k_{uni}	6.45E+01	9.60E+01	1.06E+02	1.68E+02	2.58E+02
	k_b	2.37E-18	2.40E-18	2.40E-18	2.45E-18	2.49E-18
Channel R_WQ5	K_{eq}	3.36E-21	2.67E-21	2.53E-21	1.94E-21	1.52E-21
	k_{uni}	3.75E+05	5.33E+05	5.80E+05	8.72E+05	1.28E+06
	k_b	1.26E-15	1.42E-15	1.47E-15	1.69E-15	1.94E-15
Channel R_WQ6	K_{eq}	2.24E-20	1.47E-20	1.33E-20	8.21E-21	5.21E-21
	k_{uni}	3.75E+05	5.33E+05	5.80E+05	8.72E+05	1.28E+06
	k_b	8.40E-15	7.86E-15	7.73E-15	7.15E-15	6.65E-15

[a] k_{uni} of stepwise Path R_WT2b$_1$ has been calculated according to the canonical unified statistical model described by $\frac{1}{k_{uni}(WT2b_1)} = \frac{1}{k(TS\_WT2b_1)} + \frac{1}{k(TS\_WT3b_1)}$, k(TS_WT2b$_1$) and k(TS_WT3b$_1$) is respectively the rate constants for the elementary reaction occurring through TS_WT2b$_1$ and TS_WT3b$_1$.

Table S5 The high-pressure canonical rate constant k_{total} ($cm^3 \cdot molecule^{-1} \cdot s^{-1}$) and the calculated branching ratio (β) k_{-1} (pre-reactive complex IM_WD1a$_1$ → reactants $CH_2OO + (H_2O)_2$) and k_2(pre-reactive complex IM_WD1a$_1$ → transition state TS_WD1a$_1$ → products $HOCH_2OO + H_2O$) within the temperature range of 213-320 K

T(K)	k_{-1}	k_2	$\beta(k_{-1}/k_2)$	k_{total}	k_{R_WD1a1}(CVT/SCT)
213	8.35E+04	3.97E+07	0.00	4.86E-09	4.99E-10
230	6.44E+05	7.02E+07	0.01	1.11E-09	1.68E-10
259	2.20E+07	1.53E+08	0.14	1.38E-10	3.65E-11
280	6.13E+07	2.41E+08	0.25	3.96E-11	1.47E-11
290	3.26E+08	2.91E+08	1.12	2.32E-11	9.96E-12
298	4.22E+08	3.35E+08	1.26	1.56E-11	7.45E-12
300	3.56E+08	3.46E+08	1.03	1.41E-11	6.94E-12
310	4.60E+08	4.07E+08	1.13	8.88E-12	4.95E-12
320	8.25E+08	4.72E+08	1.75	5.73E-12	3.61E-12

The high pressure canonical total rate coefficient for the reaction of CH_2OO with water dimer was calculated using MESMER program.[1] The total rate constant was calculated based on the following scheme. At first, the Criegee intermediate and water dimer are combined together to form intermediate (IM_WD1a$_1$) and this step is considered to be at equilibrium. The second step is that the formed IM_WD1a$_1$ undergo unimolecular reaction via transition state. The rate constant for the unimolecular reaction was calculated using RRKM theory with Eckart tunneling correction as implemented in MESMER program. The calculated rate constant were given in Table S5.

$$CH_2OO + (H_2O)_2 \underset{k_{-1}}{\overset{k_1}{\rightleftharpoons}} IM\_WD1_{a1}$$

$$IM\_WD1_{a1} \xrightarrow{k_2} Products$$

Based on the calculated total rate constant, the reaction between Criegee intermediate with water dimer is significantly high compared with Criegee intermediate with water monomer. The calculated rate constant is based on pre-equilibrium condition. The branching ratio (β) is the ratio between k_{-1} and k_2 was calculated and given in Table S5. Based on the branching ratio values, it will be obvious to come to the conclusion that, though the pre-equilibrium condition may not be appropriate at lower temperature (below 290 K) conditions, they become more appropriate when the temperature is above 290 K. Based on above conclusion that the pre-equilibrium approximation is appropriate above 290 K, the calculated temperature range of 290-320 K has been chosen in the whole manuscript.

Reference

2. D. R. Glowacki, C. H. Liang, C. Morley, M. J. Pilling and S. H. Robertson, *J. Phys. Chem. A*, 2012, **116**, 9545-9560.

Table S6 Rate constants (cm^3·$molecules^{-1}$·s^{-1}) of hydrogen atoms isomerization with the favorable routes for the $CH_2OO + (H_2O)_n$ (n = 2-4) reaction within the temperature range of 290-320 K[a]

T/K	k_{R_WD1a1}	k_{R_WD1a2}	k_{R_WD1a3}	k_{R_WD1a4}	k_{R_WD1}	k_{R_WD1a1}/k_{R_WD1}	k_{R_WD1a2}/k_{R_WD1}	k_{R_WD1a3}/k_{R_WD1}	k_{R_WD1a4}/k_{R_WD1}	
290	9.96E-12	8.82E-12	7.79E-12	1.12E-12	2.77E-11	0.36	0.32	0.28	0.04	
298	7.45E-12	6.42E-12	5.87E-12	8.83E-13	2.06E-11	0.36	0.31	0.28	0.04	
300	6.94E-12	5.91E-12	5.49E-12	8.35E-13	1.92E-11	0.36	0.31	0.29	0.04	
310	4.95E-12	4.53E-12	3.95E-12	6.35E-13	1.41E-11	0.35	0.32	0.28	0.05	
320	3.61E-12	3.09E-12	2.90E-12	4.92E-13	1.01E-11	0.36	0.31	0.29	0.05	
T/K	k_{R_WT1a1}	k_{R_WT1a2}	k_{R_WT1}	k_{R_WT1a1}/k_{R_WT1}	k_{R_WT1a2}/k_{R_WT1}	k_{R_WT2b1}	k_{R_WT2b2}	k_{R_WT2}	k_{R_WT2b1}/k_{R_WT2}	k_{R_WT2b2}/k_{R_WT2}
290	3.33E-12	3.22E-12	6.55E-12	0.51	0.49	7.71E-13	4.28E-13	1.20E-12	0.64	0.36
298	2.75E-12	2.83E-12	5.58E-12	0.49	0.51	6.25E-13	3.13E-13	9.38E-13	0.67	0.33
300	2.63E-12	2.75E-12	5.38E-12	0.49	0.51	5.94E-13	2.70E-13	8.64E-13	0.69	0.31
310	2.11E-12	1.61E-12	3.72E-12	0.57	0.43	4.65E-13	2.11E-13	6.76E-13	0.69	0.31
320	1.72E-12	1.15E-12	2.87E-12	0.60	0.40	3.70E-13	1.48E-13	5.18E-13	0.71	0.29
T/K	k_{R_WQ1a1}	k_{R_WQ1a2}	k_{R_WQ1a3}	k_{R_WQ1a4}	k_{R_WQ1}	k_{R_WQ1a1}/k_{R_WQ1}	k_{R_WQ1a2}/k_{R_WQ1}	k_{R_WQ1a3}/k_{R_WQ1}	k_{R_WQ1a4}/k_{R_WQ1}	
290	1.54E-13	1.16E-13	9.24E-14	3.08E-14	3.93E-13	0.39	0.30	0.23	0.08	
298	1.38E-13	1.04E-13	8.28E-14	2.76E-14	3.52E-13	0.39	0.30	0.23	0.08	
300	1.35E-13	1.01E-13	8.10E-14	2.70E-14	3.44E-13	0.39	0.29	0.24	0.08	
310	1.20E-13	9.00E-14	7.20E-14	2.40E-14	3.06E-13	0.39	0.29	0.24	0.08	
320	1.07E-13	8.03E-14	6.42E-14	2.14E-14	2.73E-13	0.39	0.29	0.24	0.08	
T/K	k_{R_WQ2b1}	k_{R_WQ2b2}	k_{R_WQ2b3}	k_{R_WQ2b4}	k_{R_WQ2}	k_{R_WQ2b1}/k_{R_WQ2}	k_{R_WQ2b2}/k_{R_WQ2}	k_{R_WQ2b3}/k_{R_WQ2}	k_{R_WQ2b4}/k_{R_WQ2}	
290	1.10E-18	3.30E-19	3.40E-19	1.83E-19	1.95E-18	0.56	0.17	0.17	0.09	
298	1.19E-18	4.46E-19	3.76E-19	1.98E-19	2.21E-18	0.54	0.20	0.17	0.09	
300	1.22E-18	6.10E-19	5.88E-19	2.03E-19	2.62E-18	0.47	0.23	0.22	0.08	
310	1.35E-18	8.75E-19	7.40E-19	2.25E-19	3.19E-18	0.42	0.27	0.23	0.07	
320	1.50E-18	1.13E-18	8.00E-19	2.50E-19	3.68E-18	0.41	0.31	0.22	0.07	

[a] k_{R_WD1a1}, k_{R_WD1a2}, k_{R_WD1a3} and k_{R_WD1a4} is the rate constants for the Path R_WD1a_1, R_WD1a_2, R_WD1a_3 and R_WD1a_4 in Channel R_WD1 (see Fig. S8); k_{R_WT1a1}, k_{R_WT1a2}, k_{R_WT2a1} and k_{R_WT2a2} is the rate constants for the Path R_WT1a_1, R_WT1a_2, R_WT2a_1 and R_WT2a_2 in Channel R_WT1 and Channel R_WT2, respectively (see Fig. S8); k_{R_WQ1a1}, k_{R_WQ1a2}, k_{R_WQ1a3} and k_{R_WQ1a4} is the rate constants for the Path R_WQ1a_1, R_WQ1a_2, R_WQ1a_3 and R_WQ1a_4 in Channel R_WQ1 (see Fig. S8); k_{R_WQ2b1}, k_{R_WQ2b2}, k_{R_WQ2b3} and k_{R_WQ2b4} is the rate constants for the Path R_WQ2b_1, R_WQ2b_2, R_WQ2b_3 and R_WQ2b_4 in Channel R_WQ2 (see Fig. S8)

Table S7 Rate constants ($cm^3 \cdot molecules^{-1} \cdot s^{-1}$) and rate ratio for the unfavorable routes of the $CH_2OO + (H_2O)_n$ (n = 2-4) reaction within the temperature range of 290-320 K[a]

T/K	k_{R_WD2}	k_{R_WD3}	k_{R_WD4}	k_{R_WT3}	k_{R_WT4}	k_{R_WT5}	k_{R_WT6}	k_{R_WQ3}	k_{R_WQ4}	k_{R_WQ5}	k_{R_WQ6}
290	5.69E-13	6.21E-18	3.55E-19	3.52E-14	1.40E-12	9.43E-15	3.91E-17	1.89E-13	2.37E-18	1.26E-15	8.40E-15
298	4.61E-13	7.36E-18	4.56E-19	3.52E-14	1.17E-12	9.55E-15	4.23E-17	1.58E-13	2.40E-18	1.42E-15	7.86E-15
300	4.38E-13	7.67E-18	4.84E-19	3.52E-14	1.11E-12	9.58E-15	4.31E-17	1.51E-13	2.40E-18	1.47E-15	7.73E-15
310	3.42E-13	9.36E-18	6.47E-19	3.53E-14	8.99E-13	9.73E-15	4.74E-17	1.22E-13	2.45E-18	1.69E-15	7.15E-15
320	2.72E-13	1.13E-17	8.51E-19	3.53E-14	7.34E-13	9.88E-15	5.18E-17	1.00E-13	2.49E-18	1.94E-15	6.65E-15
T/K	v_{WD2}/v_{WD1}	v_{WD3}/v_{WD1}	v_{WD4}/v_{WD1}	v_{WT3}/v_{WT1}	v_{WT4}/v_{WT1}	v_{WT5}/v_{WT1}	v_{WT6}/v_{WT1}	v_{WQ3}/v_{WQ1}	v_{WQ4}/v_{WQ1}	v_{WQ5}/v_{WQ1}	v_{WQ6}/v_{WQ1}
290	2.05E-02	2.24E-07	1.28E-08	5.37E-03	2.14E-01	1.44E-03	5.97E-06	4.81E-01	6.03E-06	3.21E-03	2.14E-02
298	2.24E-02	3.57E-07	2.21E-08	6.31E-03	2.10E-01	1.71E-03	7.58E-06	4.49E-01	6.82E-06	4.03E-03	2.23E-02
300	2.28E-02	3.99E-07	2.52E-08	6.54E-03	2.06E-01	1.78E-03	8.01E-06	4.39E-01	6.98E-06	4.27E-03	2.25E-02
310	2.43E-02	6.64E-07	4.59E-08	9.49E-03	2.42E-01	2.62E-03	1.27E-05	3.99E-01	8.01E-06	5.52E-03	2.34E-02
320	2.69E-02	1.12E-06	8.43E-08	1.23E-02	2.56E-01	3.44E-03	1.80E-05	3.66E-01	9.12E-06	7.11E-03	2.44E-02

[a] k_{R_WD2}, k_{R_WD3}, k_{R_WD4}, k_{R_WT3}, k_{R_WT4}, k_{R_WT5}, k_{R_WT6}, k_{R_WQ3}, k_{R_WQ4}, k_{R_WQ5} and k_{R_WQ6} is the rate constants for the Channels R_WD2, R_WD3, R_WD4, R_WT3, R_WT4, R_WT5, R_WT6, R_WQ3, R_WQ4 and R_WQ5(see Fig. S4-S6), respectively; v_{WD2}/v_{WD1}, v_{WD3}/v_{WD1} and v_{WD4}/v_{WD1} is respectively the relative rate of Channels R_WD2, R_WD3 and R_WD4 to Channel R_WD1; v_{WT3}/v_{WT1}, v_{WT4}/v_{WT1}, v_{WT5}/v_{WT1} and v_{WT6}/v_{WT1} is respectively the relative rate of Channels R_WT3, R_WT4, R_WT5 and R_WT6 to Channel R_WT1; v_{WQ3}/v_{WQ1}, v_{WQ4}/v_{WQ1}, v_{WQ5}/v_{WQ1} and $v_{WQ6}/v_{WQ1a1}$is respectively the relative rate of Channels R_WQ3, R_WQ4, R_WQ5 and R_WQ6 to Channel R_WQ1.

Table S8 Calculated concentration of water clusters (in molecule·cm^{-3}) within the temperature range of 290-320 K at different relative humidity (RH) at the ground level of the Earth's atmosphere[a]

T(K)	20% RH	40% RH	60% RH	80% RH	100% RH
			[H_2O]		
290	9.56×10^{16}	1.91×10^{17}	2.87×10^{17}	3.82×10^{17}	4.78×10^{17}
298	1.55×10^{17}	3.09×10^{17}	4.64×10^{17}	6.18×10^{17}	7.73×10^{17}
300	1.72×10^{17}	3.43×10^{17}	5.15×10^{17}	6.86×10^{17}	8.58×10^{17}
310	2.92×10^{17}	5.84×10^{17}	8.77×10^{17}	1.17×10^{18}	1.46×10^{18}
320	4.70×10^{17}	9.40×10^{17}	1.41×10^{18}	1.88×10^{18}	2.35×10^{18}
			[$(H_2O)_2$]		
290	2.36×10^{13}	9.46×10^{13}	2.13×10^{14}	3.78×10^{14}	5.91×10^{14}
298	5.44×10^{13}	2.18×10^{14}	4.90×10^{14}	8.70×10^{14}	1.36×10^{15}
300	6.50×10^{13}	2.60×10^{14}	5.85×10^{14}	1.04×10^{15}	1.62×10^{15}
310	1.63×10^{14}	6.52×10^{14}	1.47×10^{15}	2.60×10^{15}	4.06×10^{15}
320	3.71×10^{14}	1.48×10^{15}	3.33×10^{15}	5.92×10^{15}	9.24×10^{15}
			[$(H_2O)_3$]		
290	1.51×10^{11}	1.21×10^{12}	4.09×10^{12}	9.68×10^{12}	1.89×10^{13}
298	3.83×10^{11}	3.06×10^{12}	1.03×10^{13}	2.45×10^{13}	4.78×10^{13}
300	4.67×10^{11}	3.73×10^{12}	1.26×10^{13}	2.98×10^{13}	5.82×10^{13}
310	1.29×10^{12}	1.03×10^{13}	3.47×10^{13}	8.22×10^{13}	1.60×10^{14}
320	3.14×10^{12}	2.51×10^{13}	8.46×10^{13}	2.00×10^{14}	3.91×10^{14}
			[$(H_2O)_4$]		
290	1.40×10^{10}	2.23×10^{11}	1.13×10^{12}	3.57×10^{12}	8.72×10^{12}
298	3.68×10^{10}	5.89×10^{11}	2.98×10^{12}	9.42×10^{12}	2.30×10^{13}
300	4.54×10^{10}	7.26×10^{11}	3.67×10^{12}	1.16×10^{13}	2.83×10^{13}
310	1.30×10^{11}	2.09×10^{12}	1.06×10^{13}	3.33×10^{13}	8.11×10^{13}
320	3.25×10^{11}	5.19×10^{12}	2.62×10^{13}	8.29×10^{13}	2.02×10^{14}

[a] The values are reported from reference (*J. Phys. Chem. A*, 2013, **117**, 10381-10396.).

Table S9 The relative rate for the hydrolysis of CH_2OO with $(H_2O)_n$ (n = 1-4) at different relative humidity (RH)[a]

RH	T(K)	v_{WD1}/v_{WM1}	v_{WT1}/v_{WM1}	v_{WQ1}/v_{WM1}
20%	290	30.53	0.05	0.00026
	298	29.88	0.06	0.00035
	300	29.50	0.06	0.00037
	310	29.26	0.06	0.00051
	320	27.30	0.07	0.00065
40%	290	61.25	0.19	0.0020
	298	60.06	0.23	0.0028
	300	59.16	0.24	0.0030
	310	58.52	0.24	0.0041
	320	54.46	0.26	0.0052
60%	290	91.78	0.42	0.0069
	298	89.89	0.51	0.0093
	300	88.66	0.54	0.0100
	310	87.86	0.55	0.0137
	320	81.69	0.59	0.0174
80%	290	122.37	0.74	0.016
	298	119.83	0.91	0.022
	300	118.32	0.95	0.024
	310	116.48	0.97	0.032
	320	108.92	1.05	0.041
100%	290	152.89	1.16	0.032
	298	149.77	1.43	0.043
	300	147.36	1.48	0.046
	310	145.76	1.52	0.063
	320	136.00	1.64	0.080

[a] v_{WD1}/v_{WM1}, v_{WT1}/v_{WM1} and v_{WQ1}/v_{WM1} is respectively the relative rate of Channels R_WD1, R_WT1 and R_WQ1 to Channel R_WM1.

Table S10 Rate ratios of v_{WM1}/v_{total}, v_{WD1}/v_{total}, v_{WT1}/v_{total}, v_{WQ1}/v_{total}, within the temperature range of 290-320 K at different relative humidity (RH)[a]

RH	T(K)	v_{WM1}/v_{total}	v_{WD1}/v_{total}	v_{WT1}/v_{total}	v_{WQ1}/v_{total}
20%	290	0.03	0.97	0.001	0.000008
	298	0.03	0.97	0.002	0.000011
	300	0.03	0.97	0.002	0.000012
	310	0.03	0.96	0.002	0.000017
	320	0.04	0.96	0.002	0.000023
40%	290	0.02	0.98	0.003	0.00003
	298	0.02	0.98	0.004	0.00005
	300	0.02	0.98	0.004	0.00005
	310	0.02	0.98	0.004	0.00007
	320	0.02	0.98	0.005	0.00009
60%	290	0.01	0.98	0.004	0.00007
	298	0.01	0.98	0.006	0.00010
	300	0.01	0.98	0.006	0.00011
	310	0.01	0.98	0.006	0.00015
	320	0.01	0.98	0.007	0.00021
80%	290	0.01	0.99	0.006	0.00013
	298	0.01	0.98	0.008	0.00018
	300	0.01	0.98	0.008	0.00020
	310	0.01	0.98	0.008	0.00027
	320	0.01	0.98	0.009	0.00037
100%	290	0.01	0.99	0.007	0.0002
	298	0.01	0.98	0.009	0.0003
	300	0.01	0.98	0.010	0.0003
	310	0.01	0.98	0.010	0.0004
	320	0.01	0.98	0.012	0.0006

[a] $v_{total} = v_{WM1} + v_{WD1} + v_{WT1} + v_{WQ1}$

Table S11 Coordinates and geometrical structures for the stationary points in the favorable hydrolysis of CH_2OO with $(H_2O)_n$ (n = 1-4) reaction at the B3LYP/6-311+G(2*d*,2*p*) level

$CH_2OO\cdots H_2O$				**TS_WM**			
O	1.79184600	0.03264100	0.01879600	O	1.43920400	-0.38078700	-0.00701200
H	1.15741700	-0.70693900	0.10699200	H	0.54499700	-0.95182700	0.07514700
H	2.23545400	-0.10644600	-0.82133000	H	1.68892300	-0.40506600	-0.93828800
O	-0.68184300	-1.16736000	0.18575000	O	-0.95091000	-0.94342200	0.16801200
O	-0.99782500	0.05653600	-0.37878600	O	-0.88340300	0.40398400	-0.37611900
C	-0.57360700	1.07332700	0.20674100	C	0.05502500	0.99702400	0.24766200
H	-0.07143100	0.98717500	1.15940700	H	0.18944000	0.81980500	1.30604100
H	-0.77722500	2.01170700	-0.29160200	H	0.40736400	1.91674900	-0.20792300
$HOCH_2OOH$				**$CH_2OO\cdots(H_2O)_2$-a_1**			
O	1.37952500	-0.59499800	-0.01565300	O	-1.34063700	-1.42789200	-0.08278900
H	-1.18002400	-1.22727300	-0.26074100	H	-1.93493700	-1.82994400	0.55638700
H	1.70853600	-0.51936400	-0.91696200	H	-1.56041600	-0.46779600	-0.08396300
O	-1.48364700	-0.42225700	0.18273500	O	1.15584500	1.19407100	0.24735600
O	-0.61438100	0.57962800	-0.40159600	O	1.33459500	-0.00962600	-0.44940300
C	0.61277000	0.54225200	0.28655500	C	1.12995300	-1.05793200	0.18913000
H	0.44227900	0.52514500	1.36029000	H	0.89325100	-1.00526200	1.24268100
H	1.10061800	1.46899200	-0.02580400	H	1.26474200	-1.97724800	-0.36230800
				O	-1.53412400	1.29154800	0.04601100
				H	-0.55487600	1.41337700	0.12176700
				H	-1.81292400	1.82965700	-0.69874300
TS_WD1a$_1$				**IMF_WD1a$_1$**			
C	-1.30421400	0.45291600	0.11771200	C	-1.37680300	0.32529500	-0.13427100
H	-1.98490700	1.09454400	-0.42658800	H	-1.96408900	0.64408500	-0.99395600
H	-1.31468800	0.42591100	1.20037900	H	-2.01655000	0.05362100	0.70633800
O	-1.00758700	-0.62333800	-0.49493000	O	-0.68597100	-0.79871400	-0.59996700
O	-0.21376400	-1.51097000	0.34834600	O	-0.00514900	-1.39172300	0.53773700
H	0.98151700	0.90322300	-0.07152500	H	1.42490800	0.88093300	-0.31412400
O	1.85952300	-0.20877300	-0.00570300	O	2.15805500	0.29578400	-0.06940600
H	2.30416700	-0.43079100	-0.82751500	H	2.67199300	0.16121400	-0.87008200
O	0.17335000	1.60270200	-0.03428100	O	-0.52071800	1.39654400	0.22131100
H	0.28900300	2.11382400	0.77545800	H	-0.32188900	1.32773400	1.16006900
H	1.05802000	-0.90117600	0.13606100	H	0.89670900	-1.03449100	0.39998800
$CH_2OO\cdots(H_2O)_3$-a_1				**TS_WT1a$_1$**			
O	1.80154300	-1.17635600	-0.35204700	O	1.59032900	-1.10412400	-0.55295400
O	2.13850900	0.11467900	0.03229400	O	1.92442500	0.22624100	-0.07514600
C	1.55962800	1.05842500	-0.54372400	C	1.07740900	1.10276300	-0.42950200
H	0.84431800	0.85762200	-1.33502700	H	0.42088000	0.88300300	-1.26072500
H	1.84377700	2.04853600	-0.21222600	H	1.37021800	2.12154000	-0.21030400
O	-0.87890300	1.39447900	0.63952800	O	-0.42825100	1.08768800	0.79085200
H	-0.77499700	0.44375700	0.91183600	H	-0.51440700	-0.02347100	0.88959800
O	-0.66211300	-1.25077800	0.90417900	O	-0.48997900	-1.34491500	0.79807100
H	-1.34991900	-1.40138500	0.23974400	H	-1.23436800	-1.55852300	0.22158500
O	-2.77441100	-0.22390100	-0.86533400	O	-2.69633200	0.01120100	-0.70582300
H	-2.40253600	0.57151600	-0.44717800	H	-2.33922100	0.73273200	-0.17340500
H	-0.99141800	1.90362600	1.44810000	H	-0.12669500	1.43428400	1.63804800
H	0.19630700	-1.42706700	0.46237900	H	0.39709600	-1.38941700	0.21465000

H	-3.72029700	-0.21214200	-0.67424700	H	-3.63948500	0.17454800	-0.78244400
	IMF_WT1a$_1$				**$CH_2OO\cdots(H_2O)_3$-b$_1$**		
O	-0.62333800	-1.37991600	0.67718900	C	-1.71018200	1.04519600	0.40220700
O	-1.50541700	-0.80299200	-0.32072300	H	-2.04166300	1.93749000	-0.10959200
C	-1.79416800	0.50377600	0.06047300	H	-1.15616300	1.04042700	1.33252800
H	-1.93317800	0.56994400	1.13614900	O	-2.01601700	-0.03423100	-0.13995000
H	-2.71307000	0.74512000	-0.47727000	O	-1.60336500	-1.20166700	0.47514600
O	-0.77414100	1.44423300	-0.26274600	H	0.74333800	-0.46380500	-1.19764200
H	2.19646900	-1.53632100	-1.22260300	O	0.87049000	-1.38843900	-0.93466000
O	1.93204100	-1.33615200	-0.32173400	H	0.02863100	-1.60312400	-0.48833500
H	2.13547700	-0.39137200	-0.17020800	H	1.24748900	2.13875400	-1.18221800
O	1.99898000	1.36987700	0.23345600	H	1.51486100	1.20090300	0.03507900
H	1.02800800	1.45080500	0.25528700	O	0.81275500	1.54918500	-0.55704700
H	-0.72955200	1.52737000	-1.22114600	H	2.09039600	-0.78840200	0.31826900
H	0.23923300	-1.41270900	0.20263800	H	2.59390200	-0.36851100	1.72071500
H	2.31663800	1.66410400	1.09077800	O	2.59117400	-0.09546100	0.80125600
	TS_WT2b$_1$				**IM_WT3b$_1$**		
C	1.79401800	-1.02337800	0.32530500	C	-1.97184100	0.46934400	0.01290800
H	2.02821200	-1.89942500	-0.26063000	H	-2.44088300	1.12215800	-0.70822000
H	1.40884400	-1.05396300	1.33525400	H	-1.92412900	0.66925600	1.07376300
O	1.99746500	0.07103300	-0.23518000	O	-1.55894900	-0.61669100	-0.43336300
O	1.70040100	1.22776100	0.47033000	O	-1.00494400	-1.50178700	0.50487700
H	-0.90586300	1.05113400	-1.17494700	H	2.05978200	-0.06571100	-0.07926800
O	-1.05698500	1.75428200	-0.51751000	O	-0.18364800	2.16339200	0.07127100
H	-0.18042400	1.82911400	-0.09030900	H	-0.11940800	2.80516400	-0.64118300
H	-0.58422500	-2.10740000	-1.23962000	O	1.58423500	-1.71170400	-0.11973400
H	-1.36718200	-1.35911400	-0.13927600	H	1.71317400	-2.26370400	-0.89405200
O	-0.46562700	-1.61042200	-0.42540700	H	0.60920600	-1.71179000	0.06943000
H	-2.54787300	0.57905000	0.15349700	O	2.21913000	0.90520400	0.00722000
H	-3.15591500	-0.15422800	1.37244700	H	2.79157300	1.00963300	0.77116400
O	-2.85771300	-0.28576600	0.46923700	H	0.69513900	1.71162300	0.08875200
	TS_WT3b$_1$				**IMF_WT3b$_1$**		
C	1.80102500	0.05504000	-0.11630000	C	-1.79413400	0.50374300	0.06038200
H	2.69575900	0.34723200	0.42390200	H	-2.71311200	0.74483900	-0.47734300
H	1.81910000	0.10283000	-1.19766600	H	-1.93299800	0.57040500	1.13604800
O	1.20545700	-0.96003100	0.40588900	O	-1.50544700	-0.80319500	-0.32027700
O	0.26397600	-1.53985800	-0.54954700	O	-0.62302000	-1.37959500	0.67763000
H	-1.82071900	0.49105800	0.04193600	H	2.13540500	-0.39122900	-0.17046400
O	0.91669400	1.54668400	0.12130100	O	-0.77414100	1.44404000	-0.26338500
H	0.99731400	1.77578300	1.05493700	H	-0.72954700	1.52662500	-1.22183300
O	-2.01459900	-0.96043500	0.23850900	O	1.93199300	-1.33597300	-0.32226400
H	-2.23314000	-1.31410100	1.10294000	H	2.19608100	-1.53578600	-1.22331200
H	-1.04026500	-1.28621500	-0.02643800	H	0.23938700	-1.41256400	0.20279300
O	-1.52359400	1.46310100	-0.16503400	O	1.99883000	1.36985200	0.23391100
H	-1.85840300	1.68180700	-1.03901700	H	2.31601300	1.66342600	1.09163500
H	-0.14926800	1.47567100	-0.07174500	H	1.02785000	1.45079600	0.25526800
	$CH_2OO\cdots(H_2O)_4$-a$_1$				**TS_WQ1a$_1$**		
C	1.94372000	1.01875400	-0.66153500	C	1.68884100	1.02796000	-0.50100000
H	2.32349400	2.00020400	-0.41590800	H	2.10263900	1.99930200	-0.26513500

H	1.06827800	0.83575800	-1.27020100	H	0.96496700	0.89748300	-1.29284400
O	2.59640900	0.06036400	-0.20491700	O	2.40493900	0.04790400	-0.15631900
O	2.14498400	-1.21822000	-0.47671300	O	1.88659700	-1.22437000	-0.60808400
H	-0.19056500	0.48143000	1.19773800	H	-0.00134400	0.05783200	0.98851200
O	-0.25527400	1.46171200	1.00325400	O	0.14263200	1.20676200	0.79917200
H	-0.34567600	1.90690700	1.84963600	H	0.46638200	1.60760300	1.61266800
H	0.67681800	-1.37848900	0.62941100	H	0.72931200	-1.37932700	0.35756800
O	-2.48759300	-1.52086900	-0.32371900	O	-2.51292800	-1.38331400	-0.25122100
H	-2.61757800	-0.58912500	-0.58655300	H	-2.59299300	-0.42449900	-0.42319900
H	-2.53210500	-2.03832300	-1.13128400	H	-2.60230300	-1.81924200	-1.10239400
O	-0.10478800	-1.16291300	1.17783500	O	-0.05308300	-1.19336500	1.01546500
H	-0.88542400	-1.46394500	0.67620800	H	-0.89233200	-1.44971300	0.57726500
O	-2.43761000	1.25671600	-0.73851200	O	-2.33962200	1.40195900	-0.47535200
H	-1.67463000	1.32839700	-0.12961000	H	-1.52466900	1.53352900	0.04608900
H	-3.13395700	1.79034800	-0.34806000	H	-3.01098500	1.96466300	-0.08182000
	IMF_WQ1a$_1$				**$CH_2OO\cdots(H_2O)_4$-b$_1$**		
C	2.18161600	0.68310600	0.08990200	C	-1.18437600	-0.75780000	-1.12448400
H	3.07247900	0.91996700	0.67570800	H	-0.98001900	-1.73161400	-1.54691200
H	2.25897100	1.06313900	-0.92581600	H	-0.53493100	0.10516900	-1.22779700
O	2.12525400	-0.70451500	0.10783200	O	-2.25373700	-0.67611300	-0.48727900
O	1.23640100	-1.13304500	-0.95651800	O	-2.57880600	0.52970100	0.10353900
H	-1.02497600	-2.52171800	1.12930500	H	0.69021100	1.58415600	0.13765100
O	1.03486900	1.31277100	0.65384000	O	0.79220800	-1.55634700	0.89653300
H	0.91555900	0.97618500	1.54858300	H	0.94635000	-2.36609400	1.38891300
H	0.45926800	-1.46459400	-0.44832100	H	0.08061800	0.18545300	1.60946800
O	-3.02137300	-0.18550200	0.18788400	O	1.20570500	1.63874600	-0.71067500
H	-2.54020800	0.62740500	-0.07624300	H	2.46397000	0.37785900	-0.61792100
H	-3.64585700	-0.36403700	-0.51992700	H	1.33416700	2.56928600	-0.90741700
O	-1.01507700	-2.05759900	0.28964700	O	-0.23409600	1.09178700	1.46629800
H	-1.77074900	-1.43063500	0.29893800	H	-1.14244800	0.98451800	1.10664300
O	-1.44153900	1.95608700	-0.50981400	O	2.92375600	-0.47664600	-0.47127200
H	-0.54705400	1.73620800	-0.18781700	H	1.64611300	-1.30855800	0.48191200
H	-1.61540900	2.85387500	-0.21678300	H	3.76197900	-0.26240400	-0.05478300
	TS_WQ2b$_1$				**IM_WQ3b$_1$**		
C	-2.21863200	1.09279200	0.36722100	C	-2.47031635	-0.47405358	-0.03855765
H	-2.34345900	2.01422800	-0.18956200	H	-3.03684267	-0.08605858	-0.87180112
H	-1.87395900	1.03326100	1.41081900	H	-2.83407448	-0.51327857	0.97772366
O	-2.48713200	0.04813900	-0.28368000	O	-1.37428013	-0.98868845	-0.32685491
O	-2.31680800	-1.15768300	0.39257600	O	-0.65042436	-1.53399683	0.73976902
H	1.76355900	-1.78383500	-0.14718700	H	2.43983700	-0.43766700	-0.20586300
O	0.10364300	1.88692500	-0.24719000	O	-1.69360700	1.86748500	-0.30479700
H	0.02504800	2.24898700	-1.14068400	H	-1.76432500	2.32125600	-1.14885800
H	0.24261700	-1.22324500	-1.15228700	H	0.79529700	-1.89613200	0.09290600
O	2.60218200	-1.53613700	0.31145900	O	2.79000500	0.48534700	-0.17042600
H	2.84153600	0.45383700	0.26584500	H	1.56371900	1.65270900	0.18677600
H	3.32741500	-1.77720800	-0.29131700	H	3.25841200	0.62272700	-0.99712000
O	0.06389000	-1.83107100	-0.41346200	O	1.70881900	-1.98844800	-0.29153600
H	-0.83498100	-1.54615100	-0.09869400	H	2.12498800	-2.71273000	0.18138300
O	2.79583600	1.40309400	0.04049200	O	0.88352700	2.33594500	0.39489400

H	1.05449800	1.64073000	-0.11160600	H	-0.75565000	1.99584900	-0.02313400
H	3.13630615	1.44841432	-0.85943195	H	1.12012482	3.08220542	-0.16094464
	TS_WQ3b$_1$				**IMF_WQ3b$_1$**		
C	-2.18257900	-0.25945100	0.17606300	C	-2.01420400	0.62072600	-0.45572900
H	-3.12913800	-0.20328000	-0.36246900	H	-2.83836700	0.55380100	-1.17088100
H	-2.27146200	-0.31118800	1.26316900	H	-2.12094500	1.50000700	0.17992900
O	-1.39458900	-1.19309900	-0.35548900	O	-2.13832600	-0.56337800	0.27620700
O	-0.35669500	-1.45395400	0.65567000	O	-1.15884900	-0.54377900	1.34808900
H	2.16758100	-0.53163400	-0.14191700	H	1.61357500	-1.32891600	-0.32837100
O	-1.65732400	1.24233900	-0.19860100	O	-0.76725200	0.74381900	-1.11280100
H	-1.91771900	1.33410100	-1.13437400	H	-0.46125600	-0.14513900	-1.35312200
H	0.62647700	-1.59016800	0.09140500	H	-0.43344500	-1.04149900	0.91709700
O	2.51588000	0.58590300	0.24590500	O	2.99573700	-0.32118600	0.04645600
H	1.37171300	1.46763500	0.04508600	H	2.52288900	0.52612800	0.20807600
H	3.05547700	0.85926200	-0.51206700	H	3.68190200	-0.13042300	-0.59751400
O	1.76109300	-1.54664300	-0.47121000	O	0.70394600	-1.68520500	-0.45324200
H	2.22713200	-2.23722400	0.04271000	H	0.78325800	-2.63590800	-0.56279900
O	0.50397800	2.15371400	-0.00032500	O	1.33380400	1.81968000	0.42213300
H	-0.61722300	1.68600800	-0.07905200	H	0.56611300	1.51477500	-0.10235800
H	0.61877414	2.65115586	-0.81392459	H	1.70594426	2.53756291	-0.09806395